NANO LETTERS

pubs.acs.org/NanoLett Letter

Graphene/Cholesteric Liquid-Crystal-Based Electro-Driven Thermochromic Light Modulators toward Wide-Gamut Dynamic Light Color-Tuning-Related Applications

Fan Zhou,◆ Ruochen Lan,◆ Zhi Li, Bingyao Liu, Qin Xie, Jinying Bao, Junling Liu, Peng Gao, Huai Yang,* Yanfeng Zhang,* and Zhongfan Liu*

Cite This: *Nano Lett.* 2023, 23, 4617−4626 Read Online

ACCESS | Metrics & More | Article Recommendations | Supporting Information

ABSTRACT: Light filters are ubiquitous in projection and display techniques, illumination engineering, image sensing, photography, *etc.*, while those enabling wide-gamut dynamic light color tuning are still lacking. Herein, by combining the electro-heating capability of graphene and unique optical properties (thermochromism and circular dichroism) of small-molecule-weight cholesteric liquid crystal (ChLC), a brand-new thermochromic light modulator is constructed as actively tunable color filter. Transparent graphene/glass hybrid with reasonably high conductivity serves both as a high-performance heater for actuating the thermochromism of temperature-responsive ChLC and as neutral light attenuator for brightness control. Thanks to the temperature- and polarization-dependent spectral properties of the ChLC, widely tunable hue and saturation properties of transmission light color are achieved, respectively. Several intriguing applications, e.g., color-variable smart windows for backlight color tuning and color-variable filters for photography, are also demonstrated. This work hereby provides new paradigms for promoting the applications of graphene/ChLC-based light modulators in next-generation light-management-related scenarios.

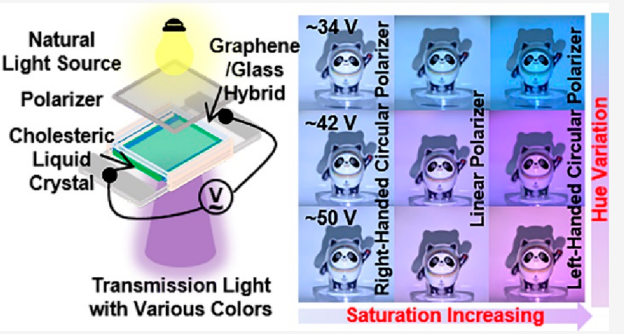

KEYWORDS: *graphene/glass hybrid, chemical vapor deposition, transparent heater, cholesteric liquid crystal, color filter, smart window*

Light color managements are ubiquitous in people's daily lives, featuring in projection and display techniques, illumination engineering, image sensing, photography, *etc.*[1,2] Thereinto, color filters are key optical elements for mediating the transmission light color, through modifying the spectral power distribution of the incident light, via various forms of light-matter interactions within the visible range (e.g., wavelength-selective absorption by dyes and pigments, scattering, reflection and/or diffraction by superstructures, and the birefringence from high-optical-anisotropy materials).[3−5] With the ever-increasing requirements on the compactness and multifunctionalization of related devices, developing actively tunable filters allowing all-around, broad-gamut light color tuning (brightness, hue, and saturation) is imperative.[2−4]

Cholesteric liquid crystals (ChLCs) have emerged as promising candidates toward this goal, due to their unique optical properties arising from the special helical arrangements of liquid crystal (LC) mesogens along the thickness direction, such as wavelength-selective reflection, circular dichroism, optical rotation, negligible absorption within the visible range, *etc.*[6−8] More significantly, their spectral properties can vary with various external stimuli (e.g., light, heat, electric field, mechanical force, various chemicals and solvents), as mainly mediated by the changes in the helical pitch (p).[9−13] This makes ChLCs very favorable for dynamically tuning the color of the transmission light.

Among these stimuli, those exerted by electricity (e.g., electric field and Joule heat) show superior stability and controllability, beneficial for precise light modulation.[14−17] So far, various electric-field- and temperature-responsive ChLC materials have been developed, including small-molecular-weight LC, polymer-stabilized LC, polymer-dispersed LC, and polymeric LC systems.[18] Among these, the small-molar-weight ones can afford faster response, broader shift of reflection band, and superior reusability, being thus more compatible with high-stability and wide-gamut light color tuning.

A high-performance transparent conductive plate is the key component in the ChLC-related devices for controllably exerting electric-related stimuli, which should possess moder-

Received: March 23, 2023
Revised: May 5, 2023
Published: May 10, 2023

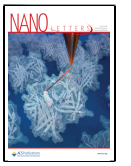

https://doi.org/10.1021/acs.nanolett.3c01118
Nano Lett. 2023, 23, 4617−4626

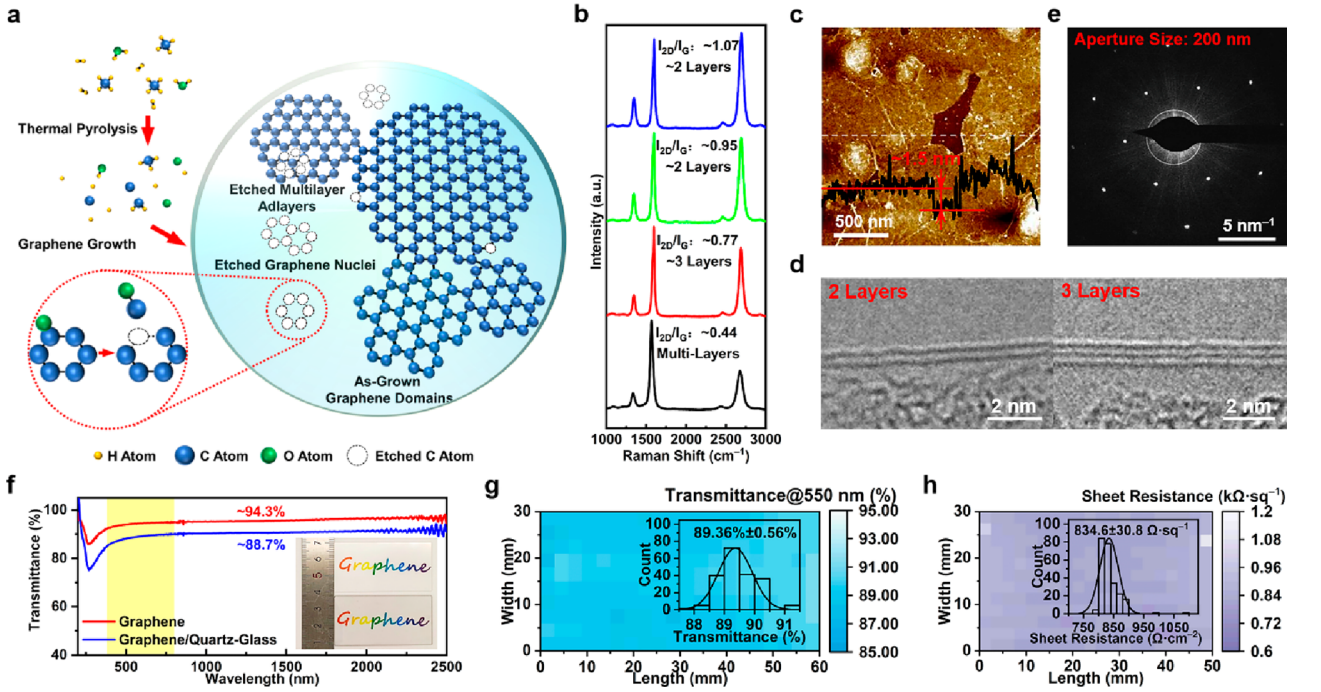

Figure 1. H_2O-assisted CVD synthesis of a large-area uniform graphene/glass hybrid with high transparency and electrical conductivity. (a) Schematic for the CVD growth of graphene on quartz glass. A tiny amount of H_2O and its pyrolysis products act as chemical etchants for reducing the nucleation density and improving the thickness uniformity of graphene films on quartz glass. (b) Typical Raman spectra collected randomly on the sample, confirming the formation of graphene. (c) Representative AFM image of graphene films transferred on SiO_2/Si. Inset: height profile along the white dashed line in (c) showing the bi- to trilayer thicknesses (~1.5 nm). (d) Typical TEM images of the graphene edges, revealing the dominant 2−3 layer thickness. (e) Sharp diffraction spots in the SAED pattern of the graphene film showing the high crystal quality. Aperture size: 200 nm. (f) UV−Vis−NIR transmission spectra of the hybrid (blue curve) and graphene film itself (red curve). Inset: photograph of a bare quartz glass piece (top) and a typical graphene/glass sample (bottom) placed on the colorful "Graphene" characters. (g) Transmittance mapping of the hybrid (to 550 nm light; 60 mm × 30 mm) and statistic histogram of the transmittance (inset, 89.4% ± 0.6%). (h) Sheet resistance mapping over the central area of the sample (50 mm × 30 mm) and the statistic histogram (inset, 835 ± 31 Ω sq^{-1}). Growth conditions: Ar/Ar+H_2O/H_2/CH_4 = 375/25/400/18 sccm, at ~1120 °C under atmospheric pressure for 6 h.

ate working voltage and a relatively high optical neutral degree. Graphene can be a perfect candidate for such purposes, considering its reasonably high transparency and electrical conductivity, and nearly wavelength-independent transmittance property within the visible range.[19−21] Moreover, its absorptivity proportional to the layer number can also enable various degrees of neutral light attenuation. Hereby, the combination of graphene and ChLC provides brand-new opportunities for multidimensional light color tuning.[22−25] Earlier, graphene films on quartz glass hybrids were used as both alignment layers and transparent electrodes, enabling reversible changes from transparent to scattering states by applying an electric field.[24] Nevertheless, wide-gamut dynamic light color tuning has yet to be realized.

This work aims to develop brand-new electro-driven thermochromic light modulators enabling dynamic light color tuning by creatively combining transparent conductive graphene/glass hybrids and thermochromic ChLC materials. Chemical vapor deposition (CVD)-derived graphene/glass hybrids with reasonably high conductivity and neutral transparency are selected as a high-performance electroheater for actuating the thermochromism of temperature-responsive ChLC. The thickness-dependent and almost wavelength-nonselective light absorption of graphene also enables different levels of nearly neutral light attenuations, favorable for brightness managements. On the other hand, temperature-responsive small-molecular-weight ChLC is elaborately designed as the color-variable light-filtering medium, based on its temperature- and polarization-dependent optical/spectral properties. Effective tuning of the hue, saturation, and brightness of the transmission light color is expected to be realized over a broad color gamut. In a further step, several practical applications of such multifunctional light modulators will also be demonstrated for the first time, including color-variable smart windows for backlight color tuning and color-variable filters for photography, *etc.*

A H_2O-assisted CVD route was developed by using methane as carbon precursor and a tiny amount of water vapor (carried by Ar gas via a bubbler) as mild etchant (~0.1 vol %, more details in Supporting Information Figures S1−S3, and Note I). According to the previous work regarding the growth of carbon nanotubes and graphene, H_2O can serve as an easily controllable oxidizer to react with carbonaceous species, through mild oxidation reactions like C (s/g) + H_2O (g) → CO (g) + H_2 (g).[26−28] Herein, the H_2O etchant and its pyrolysis products can etch away the excessive newly evolved graphene nuclei or adsorbed carbon species and the multilayer islands, beneficial for reducing the nucleation density and enlarging the graphene domain size (Figure 1a) and improving the graphene thickness uniformity. Moreover, elevated growth temperature (~1120 °C herein vs 1000−1100 °C for the conventional CVD route[22]) was also chosen to ensure improved graphitization degree. All of these designs afford improved transparent/conductive properties of the CVD-derived graphene/glass hybrids.

https://doi.org/10.1021/acs.nanolett.3c01118
Nano Lett. 2023, 23, 4617−4626

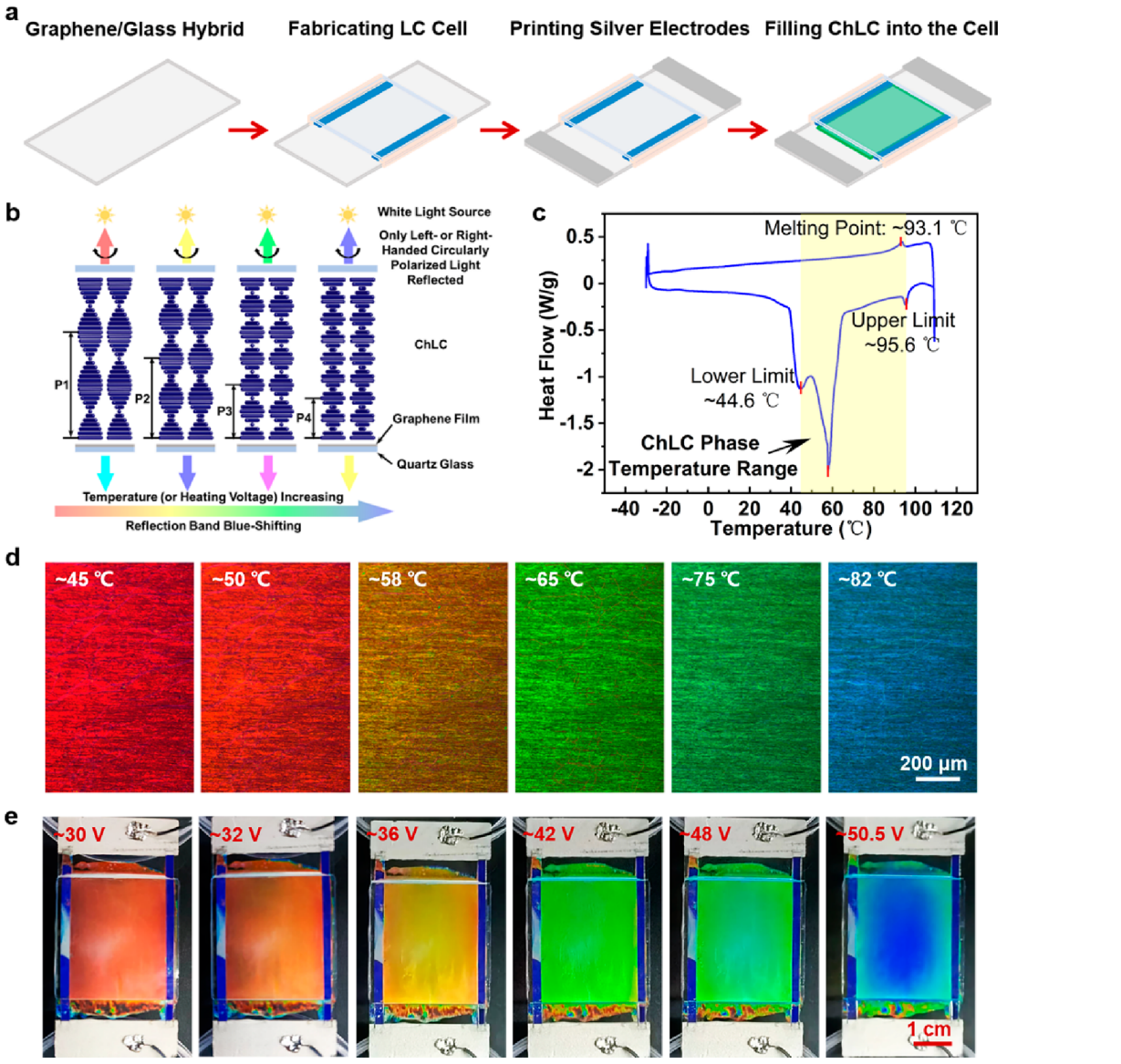

Figure 2. Fabrication of the new-type graphene/ChLC-based light modulator and its wide-gamut thermochromic property examination. (a) Schematic of the device fabrication process, including fabricating graphene/glass-based LC cell, printing silver electrodes, and filling LC monomer mixture into the cell. (b) Schematic for the temperature-dependent structural color variation of the ChLC. With rising temperature, the *p* reduces owing to the gradual smectic−cholesteric phase transition, leading to the blue shift of the reflection band and thus the gradual structural color variations from red to blue. (c) DSC curve of the ChLC sample showing the temperature range (~44.6 to ~95.6 °C) for a mesogenic state. (d) POM images of the ChLC filled into a cell under different temperatures. (e) Photographs of the graphene/ChLC-based light modulator at different applied heating voltages, showing gradual variations of the structural/reflection colors from red to blue.

According to Raman spectroscopy, the peaks at ~1580, ~2700, and ~1350 cm^{-1} correspond to G, 2D, and D bands of graphene, respectively (Figure 1b). Notably, the Raman spectra exhibit a major (~87.1%) intensity ratio of 2D to G peak (I_{2D}/I_G) of 0.7:1.2, corresponding to 2−3 layers (Supporting Information Figure S4), and minor lower I_{2D}/I_G values (e.g., ~0.44) typical for multilayer regions. Such thickness fluctuation of the graphene film is revealed by the scanning electron microscopy (SEM) characterization (Supporting Information Figure S5).[28] The 2−3 layers dominated film thickness was also precisely determined by atomic force microscopy (AFM) height profile analyses (Figure 1c, ~1.5 nm thick on SiO_2/Si) and transmission electron microscopy (TEM) characterizations (Figure 1d). Overall, relatively high graphene thickness uniformity on the quartz glass template can be achieved. The high crystal quality was also confirmed by the sharp diffraction spots in selected area electron diffraction (SAED) data. The single-crystal domain size typically exceeds the SAED aperture size (200 nm) in Figure 1e.

Optical transmission property is paramount for transparent-electrode-related applications. According to the ultraviolet−visible−near-infrared (UV−Vis−NIR) transmission spectra, the transmittance of the graphene/glass hybrid is >80% and nearly constant within 400−2500 nm (blue curve), which indicates its excellent optical transparency and neutral degree (Figure 1f and inset). Further transmittance mapping (to 550 nm light, the same hereinafter, unless stated otherwise) reveals a narrowly distributed value of 89.4% ± 0.6%, implying its macroscopic optical uniformity (Figure 1g and inset).

https://doi.org/10.1021/acs.nanolett.3c01118
Nano Lett. 2023, 23, 4617−4626

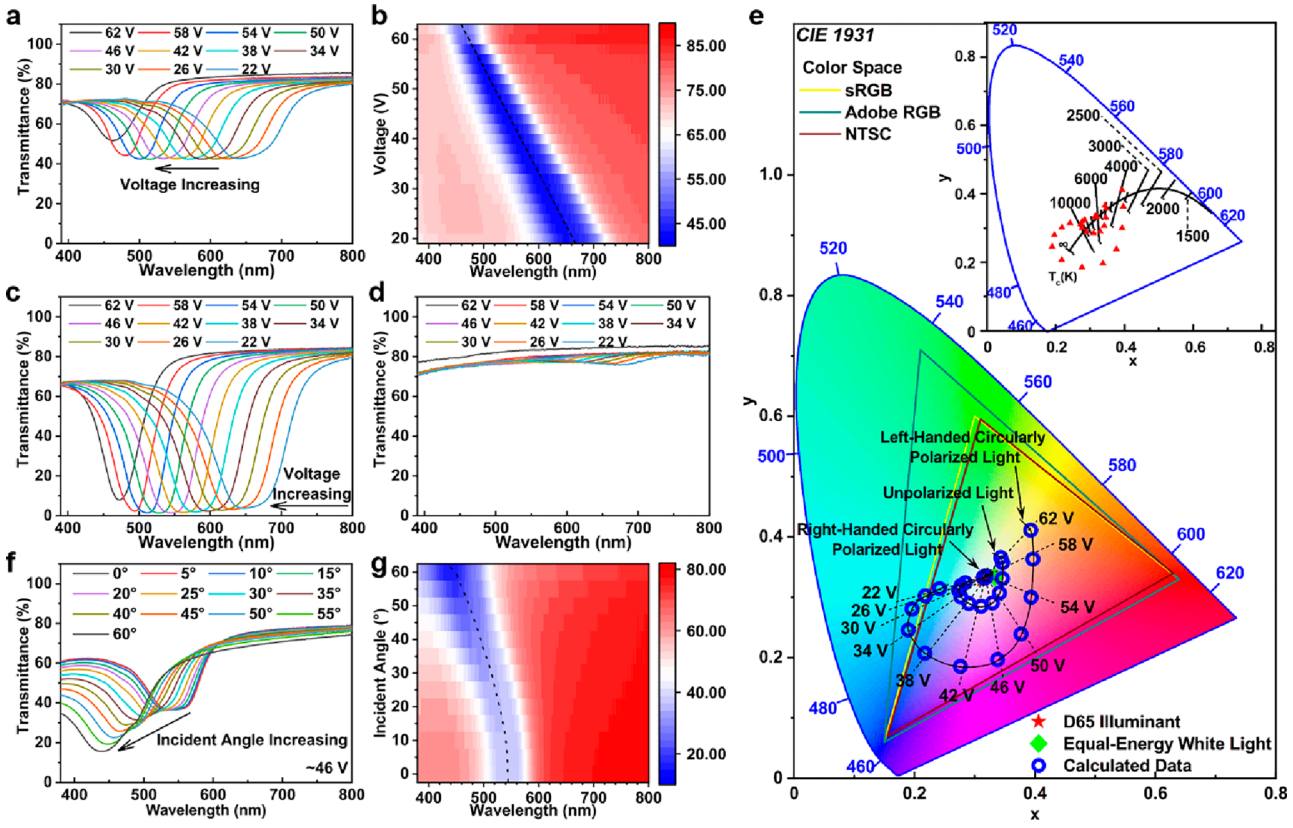

Figure 3. Highly tunable spectral properties of the graphene/ChLC-based light modulator (graphene/glass hybrid resistance: ~1.1 kΩ), at different applied heating voltages, under differently polarized incident light and various incident angles. (a, b) Heating-voltage-dependent transmission spectra (a) of the light modulator under unpolarized light and corresponding color mapping (b), showing 210 nm shift of the reflection band with increasing the heating voltage. (c, d) Transmission spectra of the light modulator under left-handed (c) and right-handed (d) circularly polarized light, showing polarization-dependent spectral property of the light modulator. (e) Color coordinates calculated from the transmittance spectra in (a, c, d) plotted in the standard International Commission on Illumination (CIE) 1931 chromaticity diagram. This plot shows the heating-voltage-dependent hue and polarization-dependent saturation of the transmission light color. Inset: correlated color temperature distribution, quantitatively showing the broad-gamut light color tuning capability of the light modulator. Simulated illuminant: D65. Standard observer: CIE 1931 2° view angle. (f, g) Incident-angle-dependent transmission spectra of the light modulator under unpolarized light at ~46 V (f) and corresponding color mapping (g). 108 nm blue-shift of the reflection band is observed with varying the incident angle from 0° to 60°.

As is known, the effects of the exerted electricity-related stimuli are closely related to the electrical conductivity of the transparent electrode. According to the sheet resistance mapping (Figure 1h and inset), a rather uniform distribution of 835 ± 31 Ω sq^{-1} is achieved, confirming the excellent macroscopic electrical uniformity of the hybrid. Notably, such a sheet resistance value (transmittance of graphene itself: ~94.3%; red curve in Figure 1f) is even ~30% lower than that of graphene grown on quartz glass (~1170 Ω sq^{-1} at ~93% transmittance) via a similar H_2O-assisted CVD route at ~1100 °C.[28]

Considering its unique optical and electrical properties, the graphene film is more suitable for fabricating ChLC-based thermochromic light modulators, with regard to a commercial indium tin oxide (ITO) film (technically controllable sheet resistance: ≤ 10^2 Ω sq^{-1}) conventionally used in LC displays. The graphene film exhibits a higher optical neutral degree than that of the ITO film, as evidenced by a much lower transmittance range (~2.9% for graphene vs ~6.7% for ITO) and narrower transmittance distribution (~94.2% ± 0.7% for graphene vs ~97.9% ± 1.5% for ITO) within the visible range (380−800 nm) (Supporting Information Figure S6). That means, compared with ITO, graphene can enable less chromaticity aberration between transmission light and incident light. Moreover, its sheet resistance value is about 1 order of magnitude higher than that of the ITO film (e.g., ~83 Ω sq^{-1} herein). Hereby, the graphene/glass-based transparent heater can afford a two times larger heating voltage range than that of its ITO/glass-based counterpart, for achieving a similar surface temperature range (~24 to ~54 V vs ~8 to ~18 V for ~40 to ~90 °C, Supporting Information Figure S7 and Note II). This should be more beneficial for finely controlling the thermochromism behavior of the temperature-responsive ChLC. Overall, the higher optical neutral degree and the more suitable sheet resistance make the graphene/glass hybrid become a better candidate in the high-performance transparent heater than its ITO-based counterpart.

A new-type electro-driven thermochromic light modulator was fabricated (Figure 2a), by utilizing the graphene/glass hybrid as a transparent heater and temperature-responsive hydrogen-bonded ChLC as thermochromic material. Herein, the LC sample was prepared by mixing the hydrogen-bonded LC monomers and chiral dopants. A graphene/glass-based LC cell was constructed with the internal gap of ~20 μm, followed by printing the silver electrodes at two ends of the LC cell. The LC sample heated to molten state was then filled into the LC cell at ~80 °C with the aid of the capillary force. The planar alignment of LC mesogens was induced by the shearing force

https://doi.org/10.1021/acs.nanolett.3c01118
Nano Lett. 2023, 23, 4617−4626

arising from the friction between the flowing LC molecules and the inner walls of the cell. Notably, left- or right-handed helically twisted superstructures of ChLC can be achieved by introducing the chiral dopants (with the derived sample denoted as left- or right-handed ChLC hereinafter, respectively). This results in selective reflection of circularly polarized light with the same handedness within a specific spectral range (known as Bragg reflection), enabling the generation of vivid structural colors.

As reported previously, the thermochromism of the hydrogen-bonded ChLC was mainly mediated by the smectic−cholesteric phase transition as well as the temperature-dependent variation of average refractive index (n_{avg}).[7,29,30] Herein, as the temperature rises, the gradual transition from the smectic to cholesteric phase promotes the winding of the helical structure, leading to the decrease of the helical pitch (p). This affords the blue shift of the reflection band, thus enabling structural color variations from red to blue, according to the Bragg equation (normal incidence) for ChLCs, $\lambda = p \times n_{avg}$ (λ: the central wavelength of the reflection band) (Figure 2b). In this work, the temperature range of the mesogenic state for the ChLC sample was determined as ∼44.6 to ∼95.6 °C via differential scanning calorimetry (DSC) characterization (Figure 2c). The broad exothermic peak centered at ∼57.9 °C can be ascribed to the transition from cholesteric to smectic phases during the cooling process.

The microscopic texture and thermochromism of ChLC were also investigated at different temperatures by performing polarizing optical microscopy (POM) characterizations on a cell filled with ChLC and placed on a high-precision heating stage. When the temperature increases from ∼45 to ∼82 °C, vivid structural color appears and varies from red, orange, yellow, green, and cyan to blue, while the uniform microscopic texture keeps nearly unchanged (Figure 2d). These results confirm the existence of the ChLC phase state within such a temperature range and its wide-gamut thermochromism property. Notably, uniformly distributed structural colors are observed throughout the whole ChLC film, indicating relatively high uniformity of the filled ChLC in centimeter scale (Supporting Information Figure S8).

By virtue of the electro-heating ability of the graphene/glass hybrid itself, similar variations of the reflection colors can also be facilely realized on the fabricated graphene/ChLC-based light modulator, by elevating the applied heating voltage from ∼30 to ∼50.5 V (Figure 2e). Exempt from an extra heater, such electro-heating mode of the new-type light modulator is perfectly compatible with various light-modulation-related applications. More importantly, the transmission light color (i.e., complementary color of reflection light color) can also be tuned accordingly, which should extend its application fields into colored illumination, smart windows, color filters, *etc.*

In general, the color of light is described by three parameters, namely, hue, saturation, and brightness, which denote the "species" (e.g., red, blue), vividness, and lightness of the light color, respectively.[31] When light passes through a medium, the color of the transmission light is closely related to the spectral property of the medium. For elaborately investigating the spectral properties of the graphene/ChLC-based light modulator, optical transmission spectra were also obtained at different applied heating voltages and under incident light with various polarization states (i.e., unpolarized, linearly polarized, and left-handed and right-handed circularly polarized light) (Figure 3). Left-handed ChLC was selected for fabricating the light modulator unless otherwise stated.

Under unpolarized light, a troughlike platform appears in the visible spectral range, corresponding to the reflection band of ChLC (Figure 3a). As the applied heating voltage increases from ∼20 to ∼62 V, the stabilized surface temperature of the light modulator rises, leading to the reduction in the helical pitch p. This allows the central wavelength of reflection band (λ) to blue-shift from ∼668 to ∼458 nm, covering most of the visible spectral range (Figure 3b). Notably, the transmittance within the reflection band is only about one-half that outside the reflection band, owing to the selective reflection of the left-handed circularly polarized component within the reflection band. Intriguingly, the transmission spectra under linearly polarized light are identical to those under unpolarized light at the same heating voltage (Supporting Information Figure S9). As for the case under left-handed circularly polarized light, an analogous heating-voltage-dependent reflection band also appears, while the transmittance within the reflection band is close to zero, owing to the nearly total reflection within such a spectral range (Figure 3c). In contrast, the transmission spectra under right-handed circularly polarized light show nearly constant transmittance (>70%) throughout the visible range, irrespective of the applied heating voltage (Figure 3d). Altogether, the spectral properties of graphene/ChLC-based light modulators highly depend on the applied heating voltages and the polarization states of incident light, in turn reflecting the thermochromism and circular dichroism of the ChLC, respectively.

The highly tunable spectral properties of the light modulator can afford transmission light with variable colors. To address this, chromaticity (i.e., hue and saturation) analyses were also performed based on the transmission spectra (Figure 3e, more details in Supporting Information Note III). According to the calculation results, under unpolarized and left-handed polarized incident light, the hue of the transmission light varies from greenish-blue, blue, purple, purplish pink, pink, and yellow-pink to orange-yellow, with increasing the applied heating voltages, which results from the blue-shift of the reflection band. At each heating voltage, the color saturation of transmission light decreases to nearly zero, by altering the incident light from left-handed circularly, linearly, and then to right-handed circularly polarized states. This can be explained by the gradually reduced transmittance difference within and outside the reflection band. Otherwise, such wide-gamut color variations can also be visualized by the broad correlated color temperature range from ∼3000 to >10000 K (inset in Figure 3e). Notably, the transmission light with other hues, such as cyan, yellow, green, *etc.*, can also be achieved by combining multiple light modulators working at different heating voltages, according to the subtractive color mixing rule (Supporting Information Figure S10 and Note IV).

More intriguingly, varying the incident angles (e.g., from 0 to 60°) can also induce blue-shift of the reflection band, thus providing another facile approach for tuning the color of the transmission light (Figure 3f,g and Supporting Information Figures S11, S12). Altogether, the color, i.e., hue and saturation, of the transmission light can be tuned over a broad gamut, by adjusting the heating voltage applied on the light modulator, incident light polarization state, incident angle, *etc.* These unique properties are beneficial for developing various wide-gamut light-modulation-related applications.

https://doi.org/10.1021/acs.nanolett.3c01118
Nano Lett. 2023, 23, 4617−4626

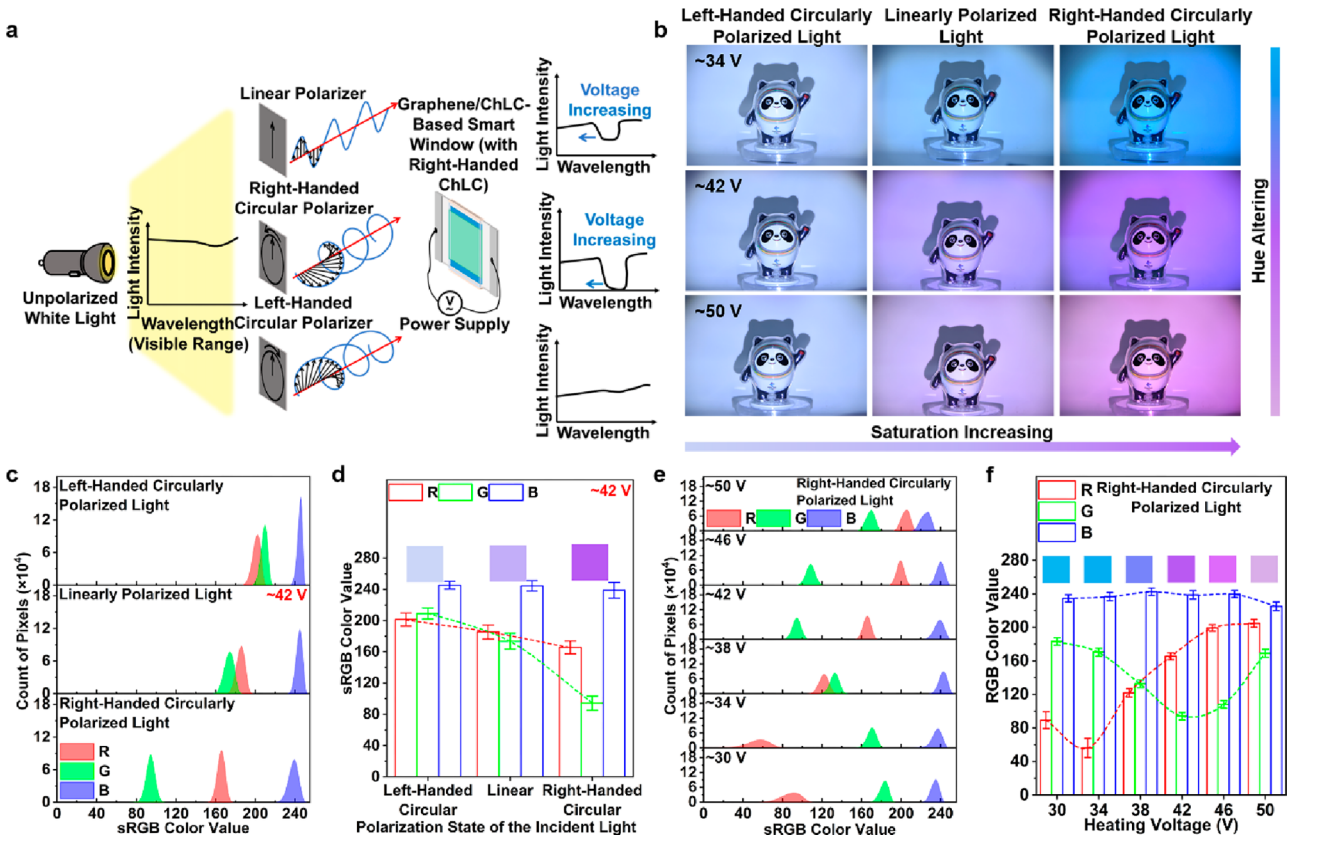

Figure 4. Applications of graphene/ChLC-based light modulators in color-variable smart windows. (a) Schematic for the working process of the graphene/ChLC-based color-variable window. When differently polarized incident light passes through the light modulator possessing a heating-voltage- and polarization-dependent spectral property, its spectral power distribution is modified. This affords transmission light with various colors, which then serves as a light source to generate backlight. (b) Photographs of the doll "Bing Dwen Dwen" (6000 × 4000 pixels) taken at different heating voltages applied on the light modulator, under left-handed circularly, linearly, and right-handed circularly polarized incident light. Heating-voltage-dependent hue and polarization-dependent saturation of the backlight colors are visually demonstrated. Aperture size: f/5.6. Exposure time: 1/20 s. (c) Histograms of sRGB color values for 1000 × 1000 pixels extracted from the background areas of the photographs under differently polarized incident light (at ∼42 V). (d) Mean values and corresponding standard deviations of sRGB color values derived from (c) through Gaussian fitting. (e) Histogram of sRGB color values for 1000 × 1000 pixels extracted from the background areas of the photographs taken at different heating voltages applied on the light modulator, under right-handed circularly polarized incident light. (f) Mean values and corresponding standard deviations of the sRGB color values derived from (e) through Gaussian fitting. The boxes above the bars in (d) and (f) display the corresponding colors searched from the sRGB color space. The heating-voltage- and polarization-dependent variations in sRGB color values shown in (c−f), which originate from the spectral property evolutions of the light modulator, account for the tunable hue and saturation of backlight colors from image analyses perspective.

The tantalizing potential in tuning the color of transmission light makes this new type of graphene/ChLC-based thermochromic light modulator promising as a wide-gamut color-variable smart window. Right-handed ChLC was employed for showing the programmable polarization selectivity of the light modulator. A white light torch was selected as the light source. The emitted unpolarized light first passes through a filter to become right-handed circularly, linearly, or left-handed circularly polarized light, with the intensity attenuated to nearly a half of its original value. When the polarized light transmits through the light modulator with heating-voltage- and polarization-dependent spectral properties, its spectral power distribution can be differently modified, affording diversified colors of the transmission light (i.e., backlight herein) (Figure 4a, more details in Supporting Information Figure S13).

For demonstrating the tunable backlight color, a doll illuminated by the transmission light was photographed, with the light modulator working at different heating voltages and under differently polarized incident light (Figure 4b and Supporting Information Figure S14a). High-transparency ChLC-free graphene/glass-based and bare quartz-glass-based cell-related devices were also fabricated as references (Supporting Information Figure S14b). Notably, brilliant backlight color is achieved under right-handed circularly polarized incident light, showing distinct variations in hue from greenish-blue, blue, purplish-blue, violet, and purple to yellowish-pink, with increasing the applied heating voltage from ∼30 to ∼50 V. Similar heating-voltage-dependent evolutions of the hue also appear under linearly polarized incident light, while the color looks less vivid, indicative of the lowered saturation. Intriguingly, the backlight under left-handed circularly polarized incident light displays a nearly neutral color of bluish-gray (close to that of the reference groups) regardless of the heating voltage, thus showing extremely low saturation. Such backlight color variations are also quantitively revealed by the standard red, green, and blue (sRGB) color value analyses (Figure 4c−f with related discussion in Supporting Information Note V and more examples in Supporting Information Figures S15−S17).

https://doi.org/10.1021/acs.nanolett.3c01118
Nano Lett. 2023, 23, 4617−4626

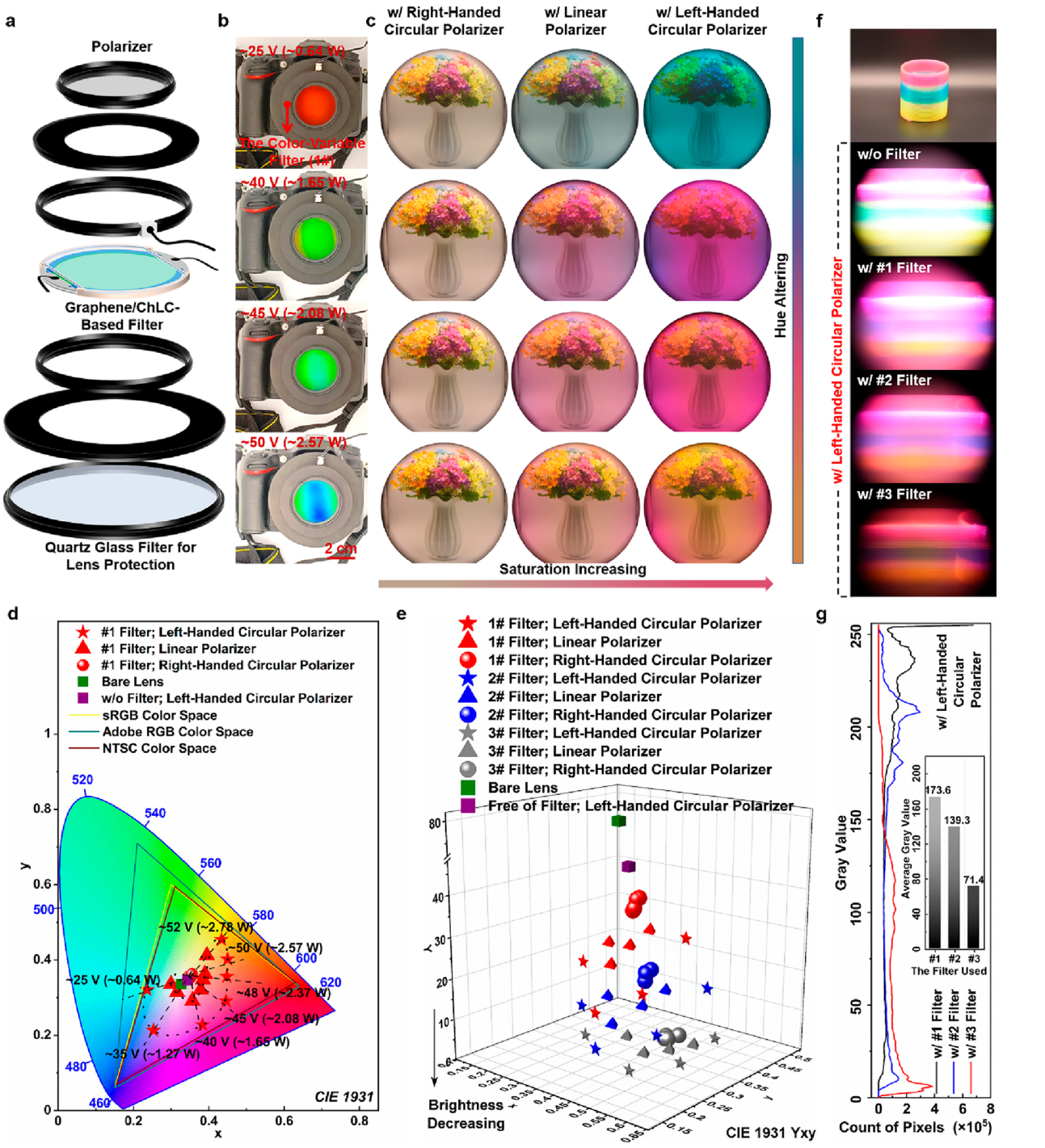

Figure 5. Applications of the graphene/ChLC-based light modulators (fabricated with left-handed ChLC) in color-variable filters for photography. (a) Schematic for the main components of the color-variable filter. (b) Photographs of the #1 filter mounted on a camera at various applied heating voltages, showing varied reflection colors from red to blue. (c) Short-exposure photographs of artificial flowers in a vase taken with the #1 filter at different applied heating voltages (powers), with right-handed circular, linear, and left-handed circular polarizers, showing the heating-voltage-dependent hue and polarization-dependent saturation of the overall backlight colors. Aperture size: f/13. Exposure time: 1/20 s. (d) CIE 1931 chromaticity diagram showing the x−y color coordinates of the backlight colors (extracted from 200 × 200 pixels, at the central area) in the photographs taken with the #1 filter at different heating voltages (powers), with different polarizers. (e) The Y−x−y color coordinates of the backlight colors in the photographs taken with #1, #2, and #3 filters (red, blue, and gray labels, respectively), at the applied heating powers of ∼0.64, ∼1.65, ∼2.08, and ∼2.57 W, with different polarizers. These results show the highly tunable hue, saturation, and brightness of the backlight colors within a broad color gamut, according to the chromaticity analyses. Those taken with bare lens (olive box) and with only a left-handed circular polarizer (purple box) are also provided as the references. (f) Photograph of a rainbow spring toy (topmost) and its long-exposure photographs (illuminated by a white torch hanging above) taken without filter and with different filters (#1, #2, and #3), at the applied heating power of ∼2.08 W (with a left-handed circular polarizer), by swinging the camera lens from left to right in photography. Aperture size: f/5.3; Exposure time: 8 s. (g) Gray value distributions and the extracted mean gray values (inset) from the central colorful areas (17867012 pixels with the same selected area shape) in the long-exposure photographs taken with filters #1, #2, and #3 filters.

https://doi.org/10.1021/acs.nanolett.3c01118
Nano Lett. 2023, 23, 4617−4626

Considering the capability of wide-gamut tuning on the transmission light color, the graphene/ChLC-based light modulators are promising for constructing portable color-variable filters in photography. Graphene/glass hybrids with different transmittances (graphene thicknesses) were selected, i.e., ∼84.4%, ∼45.1%, and ∼13.7% for #1, #2, and #3 light filters, respectively (Figure 5a, transmission spectra in Supporting Information Figure S18). A polarizer and a bare quartz glass filter were also employed for differently polarizing the incident light and for protecting the sophisticated camera lens, respectively.

Notably, with increasing the heating voltages applied on the filter from ∼25 to ∼50 V, the reflection colors at the central areas of the filters change from red, green, and cyan to blue gradually (Figure 5b). This should endow the as-taken photographs with highly tunable backlight colors complementary to reflection colors. A bunch of artificial flowers were imaged by using such filters at different applied heating voltages (powers), with different polarizers (right-handed circular, linear, and left-handed circular polarizers). Chromaticity analysis was also performed on a small central background region (200 × 200 pixels) in each photograph (Figure 5c,d, and Supporting Information Figures S19−S23 and Note III). Notably, with the #1 filter, the overall backlight colors show heating-voltage-dependent hue (from upper to lower panels) and polarization-dependent saturation (from left to right panels) (Figure 5c,d, and Supporting Information Figure S20), in good agreement with that expected from the spectra data (Figure 3). Similar hue and saturation controls were also achieved with #2 and #3 filters (Supporting Information Figures S21−S23).

Besides hue and saturation, brightness is another critical parameter for describing a color. When the filter is switched from #1 and #2 to #3, the Y coordinate (denoting the brightness of color) of the backlight color reduces from 14.5−37.4 and 6.2−19.7 to 1.1−3.1 (red, blue, and gray labels in Figure 5e, respectively, at the applied heating powers of ∼0.64, ∼1.65, ∼2.08, and ∼2.57 W). This can be ascribed to the enhanced light absorption with an increase in the graphene thickness. Intriguingly, the overall backlight colors of the photographs taken with different filters show close hue and saturation, at approximate heating power and under the same incident light (Figure 5e and Supporting Information Figure S23). These results indicate the thickness-dependent and nearly neutral light-attenuation abilities of graphene films, which contributes to controlling the exposure degree in long-exposure photography for suppressing the overexposure phenomenon (Figure 5f,g and Supporting Information Figure S24, more details and discussion in Supporting Information Note VI).

In summary, a new-type graphene/ChLC-based light modulator has been developed, by creatively integrating the electro-heating ability and nearly neutral thickness-dependent light absorption property of graphene and the temperature- and polarization-dependent spectral/optical properties (i.e., thermochromism and circular dichroism, respectively) of ChLC. This new-type light modulator enables dynamically tuning the transmission light colors (i.e., hue, saturation, and brightness) over a broad gamut. Very intriguing practical applications of such kind of light modulators are also demonstrated for the first time, such as in the color-variable smart windows for backlight color tuning, and the color-variable filters for photography. These efforts are expected to uncover the fundamental mechanisms for the new-type graphene/ChLC-based light modulators from the spectroscopy perspectives and propel their practical applications in various light-management-related scenarios. This work should also provide a brand-new paradigm for next-generation light-filtering-related devices toward functionality integration, structure compactness, and miniaturization and propel their applications in new-concept display devices, dynamic polychromatic light sources, multifunctional smart windows, *etc.*

■ ASSOCIATED CONTENT

Supporting Information

The Supporting Information is available free of charge at https://pubs.acs.org/doi/10.1021/acs.nanolett.3c01118.

Methods, supplementary schematics and characterization results regarding CVD growth of graphene films on quartz glass substrates, supplementary transmission spectra data and related chromaticity analyses, supplementary photographs and related sRGB color value analyses regarding the applications of the light modulators as the color-variable smart windows, supplementary transmission spectra data, photographs, and related chromaticity analyses regarding the applications of the light modulators in color-variable filters for photography, LC monomers for constituting the LC mixture, details for determining the volume fraction of water vapor in the gas mixture in the CVD growth of graphene, details for surface temperature measurements of the ITO/glass and graphene/glass hybrids, details regarding chromaticity analyses of transmission spectra and picture processing for extracting the color values and gray values, discussion on achieving transmission light colors with more hues by using multiple light modulators working under different heating voltages, detailed sRGB color value analyses for Figure 4c−f, and details regarding the application demonstrations of the graphene/ChLC-based color-variable filters with different graphene thicknesses in long-exposure photography (PDF)

■ AUTHOR INFORMATION

Corresponding Authors

Zhongfan Liu − *Academy for Advanced Interdisciplinary Studies and Center for Nanochemistry, Beijing Science and Engineering Center for Nanocarbons, Beijing National Laboratory for Molecular Sciences, College of Chemistry and Molecular Engineering, Peking University, Beijing 100871, P. R. China; Beijing Graphene Institute (BGI), Beijing 100095, P. R. China;* orcid.org/0000-0003-0065-7988; Email: zfliu@pku.edu.cn

Yanfeng Zhang − *Academy for Advanced Interdisciplinary Studies and School of Materials Science and Engineering, Peking University, Beijing 100871, P. R. China; Beijing Graphene Institute (BGI), Beijing 100095, P. R. China;* orcid.org/0000-0003-1319-3270; Email: yanfengzhang@pku.edu.cn

Huai Yang − *School of Materials Science and Engineering and Key Laboratory of Polymer Chemistry and Physics of Ministry of Education, Peking University, Beijing 100871, P. R. China;* orcid.org/0000-0002-3773-6666; Email: yanghuai@pku.edu.cn

https://doi.org/10.1021/acs.nanolett.3c01118
Nano Lett. 2023, 23, 4617−4626

Authors

Fan Zhou − *Academy for Advanced Interdisciplinary Studies and School of Materials Science and Engineering, Peking University, Beijing 100871, P. R. China; Beijing Graphene Institute (BGI), Beijing 100095, P. R. China*

Ruochen Lan − *School of Materials Science and Engineering and Key Laboratory of Polymer Chemistry and Physics of Ministry of Education, Peking University, Beijing 100871, P. R. China; Institute of Advanced Materials, Key Lab of Fluorine and Silicon for Energy Materials and Chemistry of Ministry of Education, Jiangxi Normal University, Nanchang 330022, P. R. China;* orcid.org/0000-0003-4802-9948

Zhi Li − *Beijing Graphene Institute (BGI), Beijing 100095, P. R. China*

Bingyao Liu − *Academy for Advanced Interdisciplinary Studies and Electron Microscopy Laboratory and International Center for Quantum Materials, School of Physics, Peking University, Beijing 100871, P. R. China*

Qin Xie − *Academy for Advanced Interdisciplinary Studies, Peking University, Beijing 100871, P. R. China; Beijing Graphene Institute (BGI), Beijing 100095, P. R. China*

Jinying Bao − *School of Materials Science and Engineering and Key Laboratory of Polymer Chemistry and Physics of Ministry of Education, Peking University, Beijing 100871, P. R. China*

Junling Liu − *Beijing Graphene Institute (BGI), Beijing 100095, P. R. China*

Peng Gao − *Academy for Advanced Interdisciplinary Studies and Electron Microscopy Laboratory and International Center for Quantum Materials, School of Physics, Peking University, Beijing 100871, P. R. China; Beijing Graphene Institute (BGI), Beijing 100095, P. R. China; Collaborative Innovation Center of Quantum Matter, Beijing 100871, P. R. China*

Complete contact information is available at: https://pubs.acs.org/10.1021/acs.nanolett.3c01118

Author Contributions

◆These authors contributed equally to this work.

Notes

The authors declare no competing financial interest.

■ ACKNOWLEDGMENTS

This work was financially supported by the National Natural Science Foundation of China (Nos. T2188101, 51925201, 52202081, and 52021006), Beijing Municipal Natural Science Foundation (No. 2214085), Beijing Municipal Science and Technology Commission Project (No. Z201100008720001), and China Postdoctoral Science Foundation funded project (No. 8206200053).

■ REFERENCES

(1) Lee, K.-T.; Seo, S.; Guo, L. J. High-Color-Purity Subtractive Color Filters with a Wide Viewing Angle Based on Plasmonic Perfect Absorbers. *Adv. Opt. Mater.* **2015**, *3*, 347−352.

(2) Ellenbogen, T.; Seo, K.; Crozier, K. B. Chromatic Plasmonic Polarizers for Active Visible Color Filtering and Polarimetry. *Nano Lett.* **2012**, *12*, 1026−1031.

(3) Gildas, F.; Dan, Y. P. Review of Nanostructure Color Filters. *J. Nanophoton.* **2019**, *13*, 020901.

(4) Nasehi, Z.; Nozhat, N. Liquid Crystal Based Tunable Plasmonic Subtractive Color Filters. *Opt. Commun.* **2019**, *445*, 96−100.

(5) Ding, B.; Zeng, P.; Huang, Z.; Dai, L.; Lan, T.; Xu, H.; Pan, Y.; Luo, Y.; Yu, Q.; Cheng, H. M.; Liu, B. A 2D Material-Based Transparent Hydrogel with Engineerable Interference Colours. *Nat. Commun.* **2022**, *13*, 1212.

(6) Bisoyi, H. K.; Li, Q. Liquid Crystals: Versatile Self-Organized Smart Soft Materials. *Chem. Rev.* **2022**, *122*, 4887−4926.

(7) Lan, R.; Wang, Q.; Shen, C.; Huang, R.; Bao, J.; Zhang, Z.; Zhang, L.; Yang, H. Humidity-Induced Simultaneous Visible and Fluorescence Photonic Patterns Enabled by Integration of Covalent Bonds and Ionic Crosslinks. *Adv. Funct. Mater.* **2021**, *31*, 2106419.

(8) Bao, J.; Wang, Z.; Shen, C.; Huang, R.; Song, C.; Li, Z.; Hu, W.; Lan, R.; Zhang, L.; Yang, H. Freestanding Helical Nanostructured Chiro-Photonic Crystal Film and Anticounterfeiting Label Enabled by a Cholesterol-Grafted Light-Driven Molecular Motor. *Small Methods* **2022**, *6*, 2200269.

(9) White, T. J.; Cazzell, S. A.; Freer, A. S.; Yang, D.-K.; Sukhomlinova, L.; Su, L.; Kosa, T.; Taheri, B.; Bunning, T. J. Widely Tunable, Photoinvertible Cholesteric Liquid Crystals. *Adv. Mater.* **2011**, *23*, 1389−1392.

(10) Chang, C.-K.; Bastiaansen, C. M. W.; Broer, D. J.; Kuo, H.-L. Alcohol-Responsive, Hydrogen-Bonded, Cholesteric Liquid-Crystal Networks. *Adv. Funct. Mater.* **2012**, *22*, 2855−2859.

(11) Stumpel, J. E.; Broer, D. J.; Schenning, A. P. H. J. Stimuli-Responsive Photonic Polymer Coatings. *Chem. Commun.* **2014**, *50*, 15839−15848.

(12) Stumpel, J. E.; Broer, D. J.; Schenning, A. P. H. J. Water-Responsive Dual-Coloured Photonic Polymer Coatings Based on Cholesteric Liquid Crystals. *RSC Adv.* **2015**, *5*, 94650−94653.

(13) Bisoyi, H. K.; Li, Q. Light-Driven Liquid Crystalline Materials: From Photo-Induced Phase Transitions and Property Modulations to Applications. *Chem. Rev.* **2016**, *116*, 15089−15166.

(14) Li, Z.; Lan, R.; Bao, J.; Hu, W.; Wang, M.; Zhang, L.; Yang, H. Tunable Circularly Polarized Luminescence with a High Dissymmetry Factor Emitted from Luminogen-Bonded and Electrically Controlled Polymer-Stabilized Cholesteric Liquid Crystals. *ACS Appl. Mater. Interfaces* **2022**, *14*, 8490−8498.

(15) Lee, K. M.; Tondiglia, V. P.; White, T. J. Photosensitivity of Reflection Notch Tuning and Broadening in Polymer Stabilized Cholesteric Liquid Crystals. *Soft Matter* **2016**, *12*, 1256−1261.

(16) Li, X. J.; Shen, Y. H.; Liu, K. R.; Quan, Y. W.; Cheng, Y. X. Recyclable CPL Switch Regulated by Using an Applied DC Electric Field from Chiral Nematic Liquid Crystals (N*-LCs). *Mater. Chem. Front.* **2020**, *4*, 2954−2961.

(17) Lu, P.; Chen, Y.; Chen, Z.; Yuan, Y.; Zhang, H. Electric Field, Temperature and Light-Triggered Triple Dynamic Circularly Polarized Luminescence Switching in Fluorescent Cholesteric Liquid Crystals with a Large Dissymmetry Factor. *J. Mater. Chem. C* **2021**, *9*, 6589−6596.

(18) Zhang, W.; Froyen, A. A. F.; Schenning, A. P. H. J.; Zhou, G.; Debije, M. G.; de Haan, L. T. Temperature-Responsive Photonic Devices Based on Cholesteric Liquid Crystals. *Adv. Photonics Res.* **2021**, *2*, 2100016.

(19) Nair, R. R.; Blake, P.; Grigorenko, A. N.; Novoselov, K. S.; Booth, T. J.; Stauber, T.; Peres, N. M. R.; Geim, A. K. Fine Structure Constant Defines Visual Transparency of Graphene. *Science* **2008**, *320*, 1308−1308.

(20) Novoselov, K. S.; Geim, A. K.; Morozov, S. V.; Jiang, D.; Katsnelson, M. I.; Grigorieva, I. V.; Dubonos, S. V.; Firsov, A. A. Two-Dimensional Gas of Massless Dirac Fermions in Graphene. *Nature* **2005**, *438*, 197−200.

(21) Chen, J.-H.; Jang, C.; Xiao, S.; Ishigami, M.; Fuhrer, M. S. Intrinsic and Extrinsic Performance Limits of Graphene Devices on SiO_2. *Nat. Nanotechnol.* **2008**, *3*, 206−209.

(22) Chen, Z.; Qi, Y.; Chen, X.; Zhang, Y.; Liu, Z. Direct CVD Growth of Graphene on Traditional Glass: Methods and Mechanisms. *Adv. Mater.* **2019**, *31*, 1803639.

(23) Chen, X. D.; Chen, Z.; Jiang, W. S.; Zhang, C.; Sun, J.; Wang, H.; Xin, W.; Lin, L.; Priydarshi, M. K.; Yang, H.; Liu, Z. B.; Tian, J.

G.; Zhang, Y.; Zhang, Y.; Liu, Z. Fast Growth and Broad Applications of 25-Inch Uniform Graphene Glass. *Adv. Mater.* **2017**, *29*, 1603428.
(24) Wang, H.; Liu, B.; Wang, L.; Chen, X.; Chen, Z.; Qi, Y.; Cui, G.; Xie, H.; Zhang, Y.; Liu, Z. Graphene Glass Inducing Multidomain Orientations in Cholesteric Liquid Crystal Devices toward Wide Viewing Angles. *ACS Nano* **2018**, *12*, 6443−6451.
(25) Cui, L.; Huan, Y.; Shan, J.; Liu, B.; Liu, J.; Xie, H.; Zhou, F.; Gao, P.; Zhang, Y.; Liu, Z. Highly Conductive Nitrogen-Doped Vertically Oriented Graphene toward Versatile Electrode-Related Applications. *ACS Nano* **2020**, *14*, 15327−15335.
(26) Yoshihara, N.; Ago, H.; Tsuji, M. Chemistry of Water-Assisted Carbon Nanotube Growth over Fe-Mo/MgO Catalyst. *J. Phys. Chem. C* **2007**, *111*, 11577−11582.
(27) Wei, S.; Ma, L.-P.; Chen, M.-L.; Liu, Z.; Ma, W.; Sun, D.-M.; Cheng, H.-M.; Ren, W. Water-Assisted Rapid Growth of Monolayer Graphene Films on SiO_2/Si Substrates. *Carbon* **2019**, *148*, 241−248.
(28) Xie, H.; Cui, K.; Cui, L.; Liu, B.; Yu, Y.; Tan, C.; Zhang, Y.; Zhang, Y.; Liu, Z. H_2O-Etchant-Promoted Synthesis of High-Quality Graphene on Glass and Its Application in See-Through Thermochromic Displays. *Small* **2020**, *16*, 1905485.
(29) Zhang, F.; Yang, D. K. Temperature Dependence of Pitch and Twist Elastic Constant in a Cholesteric to Smectic A Phase Transition. *Liq. Cryst.* **2002**, *29*, 1497−1501.
(30) Zhang, W.; Kragt, S.; Schenning, A. P. H. J.; de Haan, L. T.; Zhou, G. Easily Processable Temperature-Responsive Infrared-Reflective Polymer Coatings. *ACS Omega* **2017**, *2*, 3475−3482.
(31) Liu, Y.; Fan, Q.; Zhu, G.; Shi, G.; Ma, H.; Li, W.; Wu, T.; Chen, J.; Yin, Y.; Guan, J. A Dual Responsive Photonic Liquid for Independent Modulation of Color Brightness and Hue. *Mater. Horiz.* **2021**, *8*, 2032−2040.

https://doi.org/10.1021/acs.nanolett.3c01118
Nano Lett. 2023, 23, 4617−4626